PAPERMAKING RESEARCH SYMPOSIUM 2009
Kuopio, Finland, 1-4 June, 2009

ALIGNED ANALYSIS OF SURFACE TOPOGRAPHY AND PRINTED DOT PATTERN MAPS

M. Mettänen[1], M. Lauri[2], H. Ihalainen[3], P. Kumpulainen[4], R. Ritala[5]

[1] Corresponding author. E-mail: marja.mettanen@tut.fi,
[2] mikko.lauri@tut.fi, [3] heimo.ihalainen@tut.fi, [4] pekka.kumpulainen@tut.fi, [5] risto.ritala@tut.fi.
Tampere University of Technology, Department of Automation Science and Engineering, P.O. Box 692, FI-33101 Tampere, Finland.

Abstract. We examine the relationship between printed dot patterns and the surface topography of unprinted paper. We acquire small-scale 2D measurements of reflectance and surface topography by a camera based method and align the measurement maps obtained before and after printing. We introduce a robust two-step procedure for locating the regularly spaced raster dots from the print reflectance measurement. The first step detects the regular dot pattern with 2D Fourier analysis. The second step locates the exact dot positions by a method based on cross-correlation in the spatial domain, thus taking into account the possible deviations from the regular pattern. With the high-resolution measurements, the accurate image alignment and the detection of the dot pattern, the dependence between unprinted paper surface topography and the halftone print properties can be analyzed statistically. In this work we analyze SC paper strips of three roughness levels printed by an IGT gravure test printer under various nip pressures. Our results imply that the deep depressions in the surface topography can explain up to 15 percent of the missing or partly missing dots.

Keywords: Halftone printing, Print quality, Surface topography, 2D Fourier analysis

1 Introduction

Paper surface structure and its inhomogeneities are associated with the attainable print quality. Research on this relationship in halftone printing is particularly important because most printed matter is produced by printing dot patterns. Long before the introduction of the efficient digital image processing facilities of today, the surface profile of paper has been shown to contribute to halftone printability in letterpress [7]. Further studies on halftone prints, e.g., by Heintze et al. [6] and Bristow et al. [2], have shown the importance of the surface roughness, measured as PPS, and compressibility measurement in predicting the quality of gravure print. Later, the roughness measurements that characterize the measurement area by a single value, such as PPS, have been accompanied by 2D surface topography maps. For instance, Lipshitz et al. [12] have evaluated the distributions of various characteristics computed from high-resolution topography maps, and examined their relation to gloss. Topography maps have been acquired from paper samples before and after the application of pressure and then aligned, so that the compressibility of paper and the dependence of the number of missing gravure dots on the nip pressure in gravure printing could be studied [14]. Employing pointwise aligned 2D measurements of surface topography and fulltone print reflectance, topography has been confirmed to correlate with the small-scale gloss variation [13] and with the occurrence of missing printing ink [1, 15]. While these results clearly indicate the

statistical dependence between surface topography and print quality, the presented methods are not directly applicable to images of halftone printing that consist of ink dots instead of (intended) full coverage with the ink. The missing link is the separation of the dot areas from the void areas that lie between the dots.

In this paper we present a set of robust image analysis methods for detecting raster dot patterns from print automatically, and for studying the dependence of print defects on the surface topography of unprinted paper. To exemplify the methodology, we examine supercalendered (SC) paper samples printed by an IGT gravure test printer [8]. The area under examination is the conventional screening area of the Heliotest strip that consists of a dense regular raster dot pattern due to the engraved cells on the printing cylinder. In the printed paper some dots are partly or totally missing because of the imperfect contact between the paper and the printing cylinder. Our objective is to detect the regularity from the print reflectance image and to locate with subpixel accuracy all the coordinates where raster dots are supposed to be situated. As will be shown in Section 3, the methods developed are suitable for a wide range of prints, varying from actual halftone printing (e.g. 50 % raster) to the gravure screening that is visually very close to fulltone printing. We refer to the printed elements as raster dots in all the cases.

The problem of finding the exact dot locations falls to the area of regular pattern detection in which Fourier analysis methods are widely applied. The Fourier magnitude spectra have been recently used in [17] and [3] to extract the regular part from images of halftone printing. Vartiainen [17] has applied the method to estimate the irregular part of the image in order to detect missing dots, while Eerola et al. [3] have thresholded the synthesized regular image to locate the centroid of each dot. Our method for locating the dot coordinates also determines the average scale and the direction of the regularity from the Fourier magnitude spectrum, but each coordinate of the resulting raster point grid is refined by template matching in the spatial domain. This method is very accurate and robust against slight geometrical distortions in the image. We obtain an estimate of the expected reflectance at each pixel of the print reflectance image that would be realized if the print was perfect. We detect the pixels where printing ink is missing although they belong to the raster point area. Furthermore, we evaluate the coincidence of these defect points with the depressions in the surface topography. We also extract the raster dots from the print reflectance image and visualize their quality distribution using self-organizing maps (SOM) [11] and clustering [18].

This paper is organized as follows. We will first briefly introduce the printing experiment and the data acquisition procedure in Section 2. The search of the raster dot locations will be described in Section 3. In Section 4, we will introduce the analysis methods applied to the raster data and to the surface topography, and Section 5 will present the results. Conclusions will be drawn in Section 6.

2 Measurement data

In this work we study SC paper samples of three roughness values; in terms of PPS10 the roughness levels are 1.24 µm, 1.15 µm and 1.11 µm. For the printing experiment, the paper sheets of each roughness were cut into eight strips of width 25 mm and length 300 mm for IGT gravure test printing [8]. Three printing nip pressure levels were applied. They are presented by the printing force in Table 1 that summarizes the number of paper strips in each roughness-pressure combination. The samples were handled and printed

under standard laboratory conditions in which the temperature is 23 °C and the relative air humidity is 50 %.

Table 1: Number of paper samples in each roughness-pressure (force) combination.

	PPS10		
Printing force	1.24 µm	1.15 µm	1.11 µm
250 N	3	3	3
350 N	3	3	3
600 N	2	2	2

Before printing, we selected three test areas from the printing layout of a Heliotest strip. The first two areas, partly overlapping with each other, were in the conventional screening area that resembles visually fulltone printing, and the third area was in the beginning of the variable halftone screen area that is usually examined for the 20th missing dot [8]. The selected areas were imaged with a photometric stereo device that applies the principles described in [5]. The method is based on photographic imaging with slanting illumination and it provides reflectance and surface topography maps from exactly the same area of the paper sample. Our implementation of the measurement equipment additionally provides optical transmittance images by taking pictures of the samples with a bright illumination at the reverse side. All the images are in RGB colors and contain 2268 x 1512 pixels. The image size is 22.5 x 15 mm, and thus the pixel size is approximately 10 x 10 µm.

The imaged paper strips were printed and then the test areas were imaged again by the same procedure as before printing. The 2D measurements obtained before and after printing were aligned at subpixel accuracy by an image registration method based on cross-correlation [16]. It applies a global affine transformation [20] which, however, cannot correct the potential geometrical distortions of the image caused by the imaging optics. The distortions can be examined from the transformation fitting error map. In this experiment we observed that lens distortions larger than 0.2 pixels occur only at the edges and corners of the images and the distortions are always smaller than 0.5 pixels in the aligned images. The image registration and alignment was therefore considered accurate enough for our purpose. However, the possibility of increasing optical distortions towards the corners of the images was taken into account in the development of the dot pattern detection algorithm.

3 Dot pattern detection

The green channel of the print reflectance measurement is the most sensitive of the RGB channels to the red printing ink used in the IGT printing test. Therefore we have chosen to search for the raster dot locations from the green channel. To adapt to the possibility of the regular pattern having slightly different scale and/or direction in the opposite corners of the image, we split the print reflectance image into blocks that are processed separately. Very robust results have been obtained by using eight blocks of equal size. From each block, the dots are searched by a two-step procedure utilizing first the Fourier domain regularity information and then spatial correlations. The following two subsections will describe the steps.

3.1 Regular pattern search in 2D Fourier domain

In the first step of the raster dot localization, 2D Fourier transform is applied to the reflectance map. We apply the Welch spectrum estimate [19] with a Gaussian smoothing window to attenuate the side lobes of the peaks in the spectrum. Figure 1 (a) presents a typical spectrum estimate from a printed sample that is of relatively high quality in our IGT test printing series. A section of the corresponding print reflectance map is shown in Figure 1 (b). The spectrum peaks that can be reliably resolved from their background are located (excluding the centre peak), and their distances from each other are computed. The distances are collected into an M x 2 matrix, D, in which each row is of the form $[\Delta k_x, \Delta k_y]$, where k_x and k_y denote the wave number (in units of 1/mm) in the horizontal and vertical directions, respectively. The most frequently occurring entries in D indicate the dominating spacing of the spectrum peaks. This information is compressed by the histogram of the peak distances.

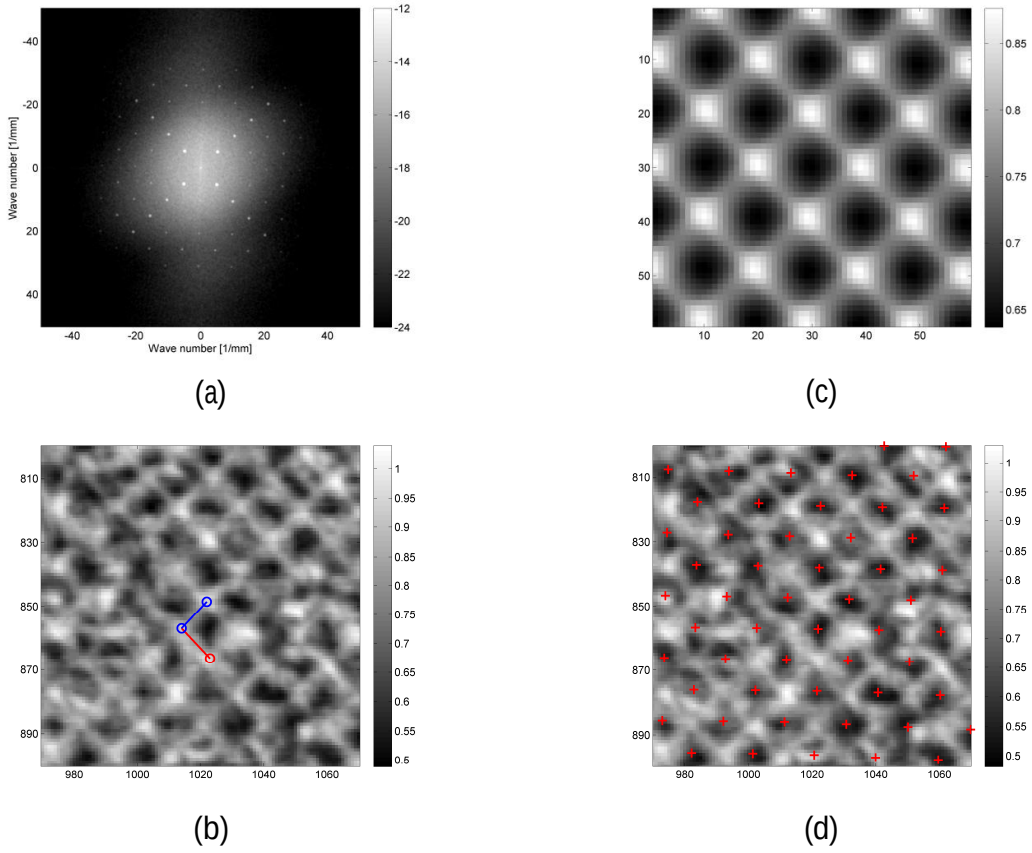

Figure 1: Raster dot search. (a) Spectrum estimate of print reflectance on logarithmic scale. (b) Found basis vectors drawn on top of a section of the print reflectance. (c) Convolution target applied in the refined search step. (d) Final grid points marked by red.

Two basis vectors are needed to determine the 2D regular structure. The first vector is determined by the entries of D that caused the highest peak in the histogram of D. The second vector is then chosen so that it does not point in the same direction as the first vector, but is still based on one of the highest peaks in D. The regular structure of the screening dot pattern is equally visible in all directions in our images, and thus the two basis vectors are found easily. They are of the form $[\Delta k_x, \Delta k_y]$. Finally the basis vectors are converted from the wave number space of the Fourier domain into spatial units (pixels). Figure 1 (b) illustrates the spatial basis vectors on top of the print reflectance map. They are duplicated in each image block to form a grid that covers the area from which the vectors were estimated. The result from the first phase of the raster dot search is thus a regular block-specific grid that indicates the average spacing of the ink dots. This grid is typically not centered to the raster dots, but that will be corrected in the second phase of the search procedure.

3.2 Refined search in spatial domain

The objective is to make the grid indicate the coordinates where the centres of the raster dots would be if they all had printed perfectly on the paper. Therefore, a large number - typically several hundred - of square shaped areas in each block are picked from around the grid coordinates provided by the first step. We define each square to cover three to four raster dots in both directions. The average of the squares, denoted as the template, represents an estimate of the average print quality in the image block. It also serves as a tool to shift the block-specific grid very close to the centres of the raster dots. In each block, we locate the centres of the raster dots in the *template* and determine the shift from the centre pixel of the template to the nearest raster dot centre. Then we apply this shift to the grid coordinates of the image block, and repeat this procedure in each block. Consequently, picking the square shaped areas from around the new grid coordinates provides a template that is centered on a raster dot. Figure 1 (c) illustrates a centered template, computed as the average of the small squares over the total image area.

The template, such as that shown in Figure 1 (c), is a prototype of the print reflectance in the paper sample. Thus we use it as a convolution target to search for similar patterns from the print reflectance map. As pointed out by Khalaj et al. [10], this self-reference method is convenient in that all the necessary information can be extracted from the image that is being analyzed, and no database is needed. The locations of maximum local correlation between the print reflectance image and the convolution target determine the final subpixel grid. By this procedure, the possible deviations from the regular pattern, caused by lens distortions, paper stretching or other reasons, are taken into consideration. The result is an accurate subpixel estimate of the location of each raster dot. Figure 1 (d) gives an example of the final grid points.

Although we have implemented the point search method using gravure printed samples as a test case, we expect it to be very useful also with other printing methods. Figure 2 presents examples of gravure and offset-printed halftone areas from which the dot locations have been successfully found by our method.

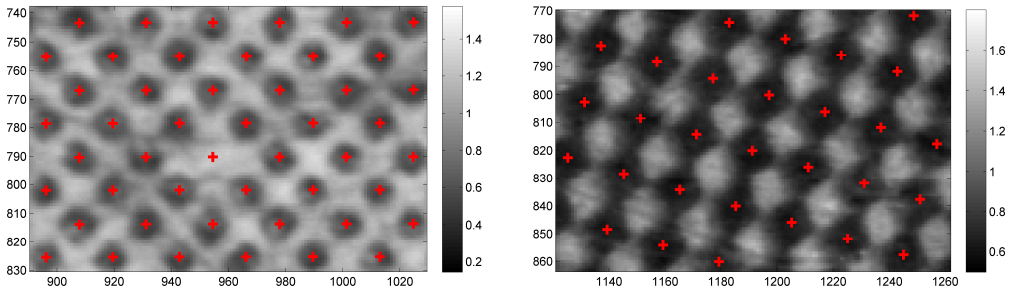

(a) (b)

Figure 2: Examples of found raster dot locations. (a) Halftone area of a Heliotest layout. (b) 50 % halftone test area of an offset-printed newspaper.

4 Analysis of printed dots

The detection of the raster pattern allows us to extract the areas of individual raster dots from the aligned print reflectance and surface topography maps. Each gravure printed sample examined in this work contains approximately 15000 dots on the 22.5 x 15 mm analysis area. This section introduces two analysis methods applied to the data. The first approach is to restrict the analysis to those points that were supposed to be covered by ink in the printing, in order to determine how large a proportion of the missing printing ink can be predicted based on the surface topography measurement. The second approach analyzes the properties of the raster dots based on their reflectance values and aims to form clusters of high and low quality dots in order to characterize the print quality.

Due to the supercalendering, some fibres on the paper surface appear dark in our topography maps, as if they were depressions. To prevent these erroneous surface height observations from affecting the analysis results, they must be removed from the analysis area. We obtain a high contrast image of the darkened fibres through the principal component analysis (PCA) [4] of the 6-dimensional image that consists of the RGB channels of the unprinted reflectance and transmittance measurements in which the fibres are also visible. By thresholding this principal component image so that 10 % of the lowest intensities are selected, we obtain a binary mask that indicates the erroneous pixels. A morphological opening operation of the mask further improves the result by reducing noise and connecting broken lines and patterns. We have made the mask to cover a rather large proportion of the image area to make sure that the number of erroneous pixels is minimized in the analysis. When the mask is applied to the grid of raster dots, slightly less than one third of the dots are discarded. Thus the number of raster dots in the analysis is still larger than 10000. This reduced data set is used throughout the analyses presented in the rest of this paper.

4.1 Coincidence of defects in topography and print

The first step in estimating the contribution of surface topography to the missing ink is to separate the pixels that belong to the ink dot area from those that lie on the void area between the dots. For this purpose the average radius of the dots is estimated from the print prototype (see Figure 1 (c)). In our work the radius is 4.5 pixels. Then, at each grid point found outside the darkened fibre area, those pixels that lie within the allowed radius

are selected from the aligned maps of unprinted surface topography and print reflectance. The pixels that lie in the regular void area of the print are not analyzed.

The overall dependence between topography and print reflectance is weak even in the restricted data set. Thus we concentrate on the tails of the probability distributions and perform a simple classification into abnormal and normal observations. The surface topography values are classified as abnormal if they are below a certain threshold, i.e., they represent abnormally deep pits or depressions. The print reflectance values are classified as abnormal if they are exceptionally high, i.e., ink is missing. The abnormal pixels of each measurement are indicated by the corresponding binary masks that have logical 1's in the abnormal points and logical 0's elsewhere. The overlap of the 1's of the topography mask and reflectance mask is then measured.

Since no ground truth is available on the amount of defects in the print or abnormalities in surface topography, we apply several mask percentages, p. For instance, the value $p = 3$ % means that three percent of the pixels that were found valid for the analysis purposes are marked abnormal. They correspond to the tail of the distribution of the measurement values. The same mask percentage is always applied to both the topography and print reflectance measurements. The value of p varies in this work from 0.5 % to 15 %. The probability of accidental coincidence of the topography and reflectance masks obviously increases linearly with p. Therefore we subtract the value of p from the computed overlap percentage.

4.2 Analysis of print quality with SOM and clustering

Self-organizing map (SOM) [11] and clustering [18] are used to detect representative samples of the main characteristics of the raster dots. In this case, the individual raster dots are extracted from the print reflectance map as square shaped areas from around the valid grid coordinates and interpolated to have their exact centre points in the middle pixel of the square. The size of each square is 13 x 13 pixels. In high quality raster dots, printing ink is expected to appear in the middle as a dark, round area of diameter 9 pixels.

The SOM with 200 nodes is first trained using six features computed from the print reflectance data: the overall mean and standard deviation in the raster dot, and the mean values and standard deviations in the inner and outer circular partitions of the dot. In this study we use a 1-dimensional SOM which is initialized along the first principal component of the 6-dimensional feature space [9]. Using SOM as an intermediate step reduces the computational load. It also helps in visualizing the results. SOM arranges the nodes along a line by their proximity. Due to the initialization by PCA, the poor and high print quality dots tend to be organized in the opposite ends of the line providing a plausible interpretation of the results. These data do not have distinct clusters but spread out smoothly in the data space. However, hierarchical clustering with complete linkage [9] applied to the code vectors of the 1-dimensional SOM has shown to reveal useful clusters. We have chosen to form ten clusters. The mean values and standard deviations of the raster dots within each cluster are calculated to represent the main characteristics of the clusters. Finally, the similar data selection procedure as described above is performed on the aligned surface topography map, and the mean values and standard deviations of the topography selections are calculated in the clusters that were determined based on the print reflectance. Examples of the results will be given in the following section.

5 Results

The analysis of the aligned topography and reflectance measurements reveals the degree to which the surface topography has been the reason for missing ink. An earlier study with fulltone test areas has found 7 % to 18 % overlap between missing ink and the surface depressions in offset printing [15]. Figure 3 presents our results from the gravure printing experiment. They are comparable with those of the offset trial, except for the smoothest paper quality. The abnormally deep points in the surface topography of the unprinted SC paper seem to have some ability to predict the missing ink. Figure 3 also shows that the predictive power increases with increasing printing nip pressure. This implies that the surface depressions - at least in SC paper - are not as sensitive to increasing nip pressure as the other factors that explain missing ink. By visual assessment, the increasing nip pressure clearly improves the print quality.

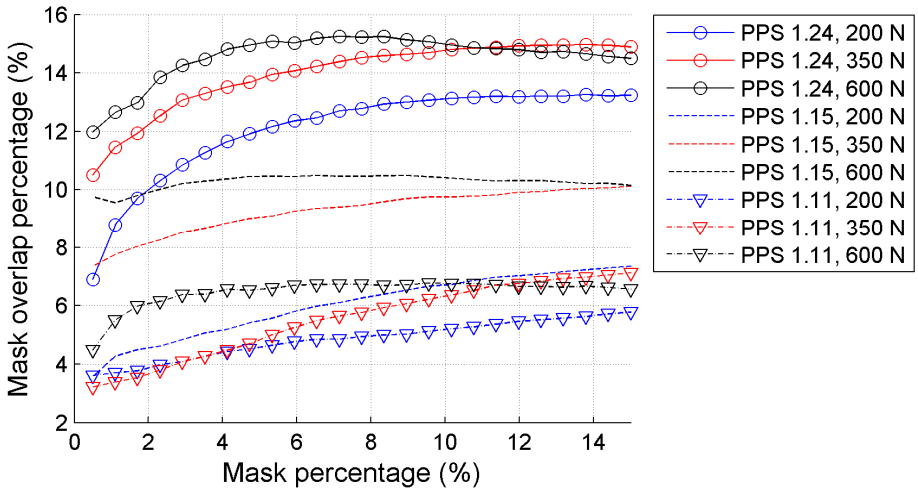

Figure 3: Overlap of the masks of missing ink and topography depressions. Each curve presents the average of two or three test areas as depicted in Table 1. The mask percentage, *p*, has been subtracted from each curve.

SOM and clustering have been applied to the raster dots to form clusters that characterize the quality of the print. The clusters are based on the print reflectance measurement but the surface topography of the unprinted paper is also examined inside the clusters formed. Figures 4 and 5 illustrate typical results from the opposite ends of the range of tested conditions (in terms of paper roughness and printing pressure). In the high print quality sample presented in Figure 4, approximately 80 % of the raster dots can be considered to have printed successfully. They are contained in five clusters that are also characterized by smooth surface topography free of deep depressions. A few small clusters on the right present raster dots with ink missing in the centre, and the mean values of surface topography in these clusters imply pits of the same size scale. These clusters cover 4-7 % of the raster dots, which is also in line with the overlap percentage of abnormalities presented in Figure 3.

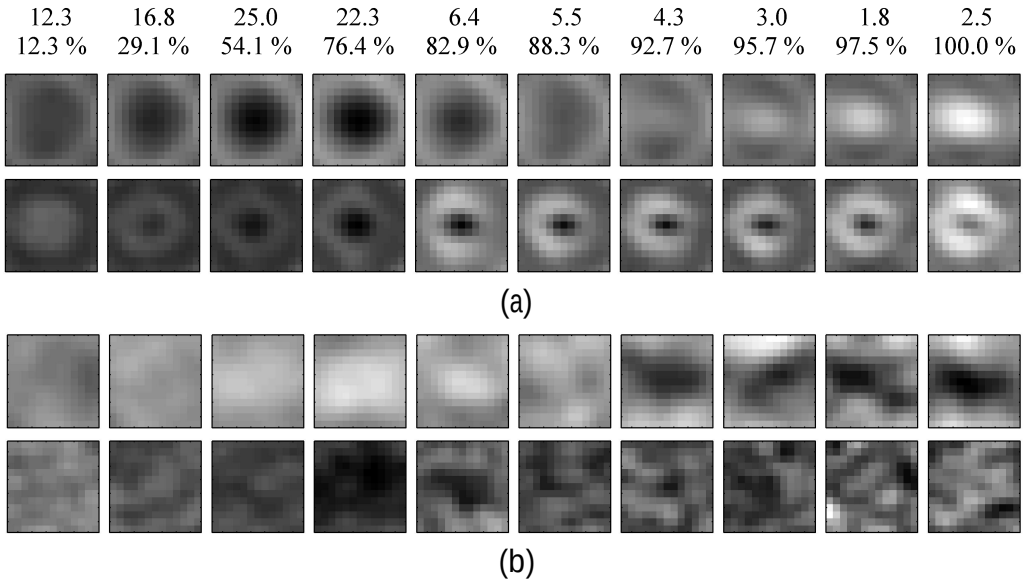

Figure 4: Raster dot clusters from a smooth paper (PPS 1.11 µm) printed at the highest pressure (force 600 N). The percentages of raster dots falling into each cluster, as well as the cumulative percentages, are given at the top. (a) Print reflectance, showing the mean of the raster dots in each cluster in the top row and the standard deviations in the bottom row. (b) Corresponding mean and standard deviation from unprinted surface topography.

Figure 5 presents the clustering results for one of the lowest quality paper samples of the test. In this sample, only 30-40 % of the raster dots are of high quality. The low standard deviation in the middle of the raster dots in several clusters also confirms that missing ink is very common in this sample. Similarly to Figure 4, the deep depressions of surface topography mainly appear in the clusters on the right, where the clusters seem to have formed due to clearly missing ink or variable quality of raster dots.

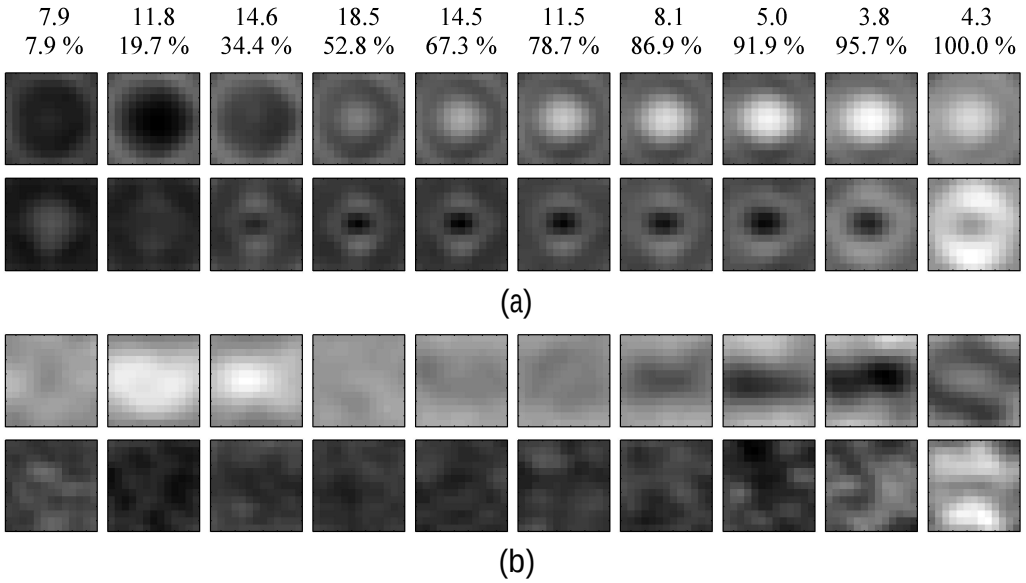

Figure 5: Raster dot clusters from the roughest paper (PPS 1.24 µm) printed at the lowest pressure (250 N). (a) Print reflectance, (b) Surface topography. See Figure 4 for details.

6 Conclusion

In this work we have examined the occurrence of missing or partly missing raster dots and their relation to the surface topography of unprinted paper. We have demonstrated the developed tools with SC paper samples printed by an IGT gravure test printer. To analyze the correspondence between surface topography and print reflectance, it is necessary to identify the dot locations. We have proposed a new method to locate robustly the subpixel coordinates of the raster dots and used the found coordinates to extract the raster dots from the print reflectance images.

We have found that the depressions in the surface topography moderately predict the missing ink in this gravure printing experiment. At maximum, 15 % of the exceptional surface depressions coincide with the locations of missing ink. As expected, this happens with the roughest SC sample used in the test. The effect of increasing printing nip pressure has also been studied, and the results imply that the pressure increase slightly improves the probability of finding missing ink from points that have been detected as surface depressions. However, the roughness of the paper samples has a larger impact on this predictive capability than the pressure. Applying SOM and hierarchical clustering to the raster dots has shown to be an efficient method for visualizing the large data set and for characterizing the print quality. The connection between small but deep paper surface depressions and missing printing ink is also visible in the clustering results, which encourages to use this method in the future analyses of paper surface properties and halftone print quality.

References

[1] Barros, G.G.: Influence of substrate topography on ink distribution in flexography. Ph.D. thesis, Karlstad University (2006)

[2] Bristow, J.A., Ekman, H.: Paper properties affecting gravure print quality. TAPPI Journal, 64(10):115-118 (1981)

[3] Eerola, T., Kämärainen, J.-K., Lensu, L., Kälviäinen, H.: Visual print quality evaluation using computational features. In: G. Bebis et al. (eds.) Proceedings of the 3rd International Symposium on Visual Computing (ISVC 2007). Part I, pp. 403-413, Lake Tahoe (2007)

[4] Geladi, P., Grahn, H.: Multivariate Image Analysis, John Wiley & Sons, Chichester (1996)

[5] Hansson, P., Johansson, P.-Å.: Topography and reflectance analysis of paper surfaces using a photometric stereo method. Optical Engineering 39(9):2555-2561 (2000)

[6] Heintze, H.U., Gordon, R.W.: Tuning of the GRI proof press as a predictor of rotonews print quality in the pressroom. TAPPI Journal, 62(11):97-101 (1979)

[7] Hendry, I.F.: Some techniques for the assessment of coated art papers. TAPPI Journal, 44(10):725-731 (1961)

[8] IGT Testing Systems: IGT Information leaflet W41 (2003)

[9] Johnson, R.A., Wichern, D.W.: Applied multivariate statistical analysis, 4th ed., Prentice-Hall, Upper Saddle River (1998)

[10] Khalaj, B.H., Aghajan, H.K., Kailath, T.: Patterned wafer inspection by high resolution spectral estimation techniques. Machine Vision and Applications, 7(3):178-185 (1994)

[11] Kohonen, T.: Self-Organizing Maps, Series in Information Sciences, Vol. 30, Springer, Heidelberg (1995)

[12] Lipshitz, H., Bridger, M., Derman, G.: On the relationships between topography and gloss. TAPPI Journal, 73(10):237-245 (1990)

[13] MacGregor, M.A., Johansson, P.-Å., Béland, M.-C.: Measurement of small-scale gloss variation in printed paper. In: Proceedings of the 1994 International Printing and Graphic Arts Conference, pp. 33-43, Halifax (1994)

[14] Mangin, P.J., Béland, M.-C., Cormier, L.M.: A structural approach to paper surface compressibility - relationship with printing characteristics. In: C.F. Baker (ed.) Transactions of the 10th Fundamental Research Symposium, Vol. 3, pp. 1397-1427, Oxford (1993)

[15] Mettänen, M., Hirn, U., Lauri, M., Ritala, R.: Probabilistic analysis of small-scale print defects with aligned 2D measurements. Accepted for publication in: Transactions of the 14th Fundamental Research Symposium, Oxford (2009)

[16] Mettänen, M., Ihalainen, H., Ritala, R.: Alignment and statistical analysis of 2D small-scale paper property maps. Appita Journal, 61(4):323-330 (2008)

[17] Vartiainen, J.: Measuring irregularities and surface defects from printed patterns. Ph.D. thesis, Lappeenranta University of Technology (2007)

[18] Vesanto, J., Alhoniemi, E.: Clustering of the self-organizing map. IEEE Transactions on Neural Networks, 11(3):586-600 (2000)

[19] Welch, P.D.: The use of Fast Fourier Transform for the estimation of power spectra: A method based on time averaging over short, modified periodograms. IEEE Transactions on Audio and Electroacoustics 15(2):70-73 (1967)

[20] Wolberg, G.: Digital Image Warping, IEEE Computer Society Press, Los Alamitos (1990)